CONF-970738--4

BNL-64293

THE EFFECT OF Ru AND Sn ADDITIONS TO Pt ON THE ELECTROLCATALYSIS OF METHANOL OXIDATION : AN INSITU XAS INVESTIGATION

Sanjeev Mukerjee and James McBreen
Department of Applied Science, Material Science Division
Brookhaven National Laboratory
Upton, New York, 11973, USA

ABSTRACT

Elements such as Ru and Sn used as ad-atoms or as alloying elements are known to enhance methanol oxidation reaction (MOR). Ru, both as alloying element as well as upd deposited on Pt/C is widely acknowledged for enhancing MOR. Sn on the other hand is more controversial, with evidence indicating enhancements for MOR when present as upd layer and marginally effective when present as an alloying element. In situ XAS is used to investigate some of these inconsistencies in the electrocatalysis of MOR. Results indicate that alloying Sn with Pt (Pt_3Sn primary phase) causes partial filling of the Pt 5 *d-band* vacancies and increase in the Pt-Pt bond distances which is directly opposite to a similar situation with Ru. Upd Sn however does not perturb Pt structurally or electronically. Ru and Sn (both as alloying element and as upd ad-layer) are associated with oxygenated species, the nature and strength of the Ru and Sn - oxygen interactions are potential dependent. Hence alloying with Sn renders Pt surface unfavorable for methanol adsorption in contrast to alloying with Ru. Both Ru and Sn however promote MOR via their ability to nucleate oxygenated species on their surface at lower potentials as compared to pure Pt.

1. INTRODUCTION

Electrocatalytic effects of adding Ru and Sn to Pt has been studied for their ability to enhance electro-oxidation of methanol, CO and other C_1 compounds in the past three decades due to their potential use in fuel cells. Early work on these electrocatalysts specially at Shell Research has been reviewed by McNicol [1,2]. Work during the eighties has been reviewed by Léger & Lamy [3] and Parsons *et al.*, [4]. Reports on enhancement of the activity of methanol electro-oxidation by PtRu systems relative to Pt have been consistent regardless of the mode of preparation (alloyed, ad-atoms *etc.*,) and testing. However, the literature on the effect of Sn as a promoter of methanol oxidation is shrouded in inconsistencies. Most of the earlier reports [5-11] have reported enhanced activity compared to Pt. However, others [12-14] have reported little or slightly lower activities compared to Pt. The source of these inconsistencies is the variety of methods used to add Sn to Pt, ranging from (*i*) electrochemical co-deposition (*ii*) upd Sn additions (*iii*) alloy formation, *etc.*, and hence in the state of the bimetallic catalyst. Majority of the reports related to enhancements in electrode kinetics involve electrocatalysts where Sn is not alloyed to Pt (such as in upd deposition). Most of the studies related to bulk Pt-Sn alloys,

specially the Pt_3Sn phase [12-13] have reported little or no enhancements. In contrast however is a report of enhanced activity in carbon supported PtSn alloy electrocatalysts containing primarily Pt_3Sn phase (minor phase being PtSn) [15]. Besides these inconsistencies, it has also been reported [16] that Pt_3Sn bulk alloy is more active for CO electro-oxidation than PtRu alloy. Hence the apparent paradox : PtSn alloy is a good electrocatalyst for CO electro-oxidation but apparently not for methanol, but upd Sn on Pt has been consistently reported for its enhanced activity for methanol oxidation. PtRu alloys on the other hand are consistently reported to be good electrocatalysts for both CO and methanol oxidation. This is in context to the overwhelming evidence for the pathway of methanol oxidation which points to Pt surface poisoning due to the formation of CO and CHO moieties and the bifunctional mechanism, based on the ability of the more oxidizable element to nucleate OH species at lower potentials as compared to Pt thereby initiating their oxidation at more negative potentials relative to Pt.

In this investigation we have examined the effect of addition of Sn (both as an alloy and as a upd layer) and Ru to Pt from the point of view of the changes brought about in the electronic and structural characteristics of Pt under *in situ* electrochemical conditions in order to address some of the issues discussed above. X-ray absorption spectroscopy offers the unique ability to simultaneously probe both the electronic and geometric parameters under *in situ* electrochemical conditions and with element specificity. The ability to probe the L absorption edges (*p-d* transitions) of Pt under *in situ* conditions using the near edge part of the spectra (X-ray absorption near edge structure, XANES) provides a direct measure of Pt *5 d*-band vacancies/atom. Besides this, both the L and K edge XANES spectra can provide information on the changes in the oxidation state, perturbation of the electronic states due to adsorption of OH, H and C_1 species and corrosion/dissolution of the absorbing element. The post edge region of the spectrum (up to 1500 eV beyond the edge, referred to as the extended X-ray absorption fine structure, EXAFS) provides the short range atomic order (bond distances, coordination numbers *etc.*).

2. EXPERIMENTAL

The carbon supported Pt, PtSn and PtRu alloys were obtained from ETEK Inc., (Framingham, MA, USA). They all had the same metal loading of 20 percent on Vulcan XC72 carbon black (Cabot Corp., USA). Underpotential deposition of Sn on Pt was carried out using a 3mM $SnCl_4$ solution in 1 M $HClO_4$ and potentiostatically polarizing it at 330 mV vs RHE for 3.75 hrs. The alloys contained 50 weight percent Pt : alloying element. X-ray powder diffraction studies on the Pt and Pt alloy electrocatalysts were done using beam line X27A at the National Synchrotron Light Source (NSLS). Details of the optics of this beam line and diffraction analysis are given elsewhere [17]. Electrodes were prepared using a standard vacuum table paper making technique described in more detail elsewhere [18]. All electrodes were soaked for 48 hrs in 1 M $HClO_4$ to achieve complete wetting, an essential requirement for conducting transmission XAS. The electrolyte of choice for these experiments was $HClO_4$ due to lack of adsorption of its anion in contrast to H_2SO_4 *etc.*, a property similar to perfluorinated polymer electrolytes. Details of the *in situ* spectro-electrochemical cells are given elsewhere [19]. XAS experiments were conducted at NSLS using beam lines X23A2 and X11A. XAS measurements were taken at Pt L_3 and L_2 edges, together with K edge of the alloying elements Sn and Ru at a variety of potentials using a sweep rate of 2mV/s for transitions between them. Methodologies adopted for data acquisition,

beam line optics, monochromator resolutions, XANES and EXAFS data analysis are given elsewhere in detail [18-20].

3. RESULTS AND DISCUSSION

3.1. X-ray Diffraction and Electrochemical Characterization

Synchrotron radiation set at 24.4 KeV (λ=0.505 Å) were used for X-ray powder diffraction patterns of Pt and Pt alloys in order to provide high resolution spectra for particle size analysis. Lattice parameters for the alloys, found after indexing the peaks to a Pt_3M type lattice (Pm3m for PtSn and PtRu) with fcc structure are given in Table 1 together with the Pt-Pt bond distance. It is interesting to note that while PtRu/C alloy results in a lattice contraction, the PtSn/C alloy results in an expansion. The particle size was determined, applying the Scherrer equation to the FWHM of the principle <111> diffraction peaks for Pt and Pt alloys. The particle sizes were found to be in the range of 34-35 Å. The values of these particle sizes agree well with independent measurements conducted using TEM analysis by ETEK Corp., as well as previous investigations such as those on PtRu/C (ETEK, same composition) [21].

Figure 1 (a) shows the cyclic voltammogram for Pt/C in 1 M $HClO_4$ with and without 0.3 M MeOH in the *in situ* spectro-electrochemical cell using a scan rate of 2mV/s. As evident from this figure, the onset of methanol oxidation during the anodic scan starts at ~ 0.5 V vs. RHE. In contrast to this the Ru alloyed to Pt (PtRu/C) initiates the oxidation ~ 100 mV negative to this, besides showing an enhancement one order of magnitude higher (Fig. 1 (b)). Similarly, the addition of Sn to Pt also enables the initiation of methanol oxidation at 100 - 120 mV negative to the Pt/C electrocatalyst. In addition, comparison of the upd Sn on Pt/C and PtSn/C alloy electrocatalyst show that the upd Sn is able to enhance methanol oxidation up to 4 times more than the alloyed electrocatalyst (Fig. 1 (c)). The coverage by ad-atoms of Sn on Pt (θ_{Sn}) was found to be 0.76 and was determined using methodology discussed in detail elsewhere [11]. These results agree well with the wealth of previous reported literature discussed in section 1. It is recognized however that these measurements are dynamic and hence provide a qualitative picture; for quantitative comparisons static Tafel type electrochemical tests need to be carried out. However, the general trend is clear and provides confirmation of the apparent paradox in the activity differences of PtSn electrocatalyst dependent on the nature of its interaction with Pt. In order to better understand this *in situ* XANES and EXAFS measurements were carried out in the same spectro-electrochemical cells at Pt L and the Ru and Sn K edges.

3.2. XAS analysis at the Pt L edge for Pt/C.

Figure 2 (a) shows the XANES at the Pt L_3 edge for Pt/C in 1 M $HClO_4$. As evident from this figure, there is considerable perturbation of the magnitude of the spectra (white line) in the regions of hydrogen adsorption/desorption and oxide coverage. This manifests itself as widening near the high energy side of the peak at 0.0 V and increase at 0.84 V. At 0.54 V (double layer region) the spectra is very close to that of the Pt reference foil. Such perturbations as a function of potential has been discussed in detail elsewhere [19, 22]. Briefly, the widening at 0.0 V is attributed to formation of unoccupied states on the high energy side of the Fermi level due to hydrogen adsorption. At 0.84 V the considerable increase in the white line is due to adsorption of

oxygenated species. The corresponding changes in the Pt *5d-band* vacancies/atom are given in Table 2. EXAFS spectrum at the Pt L_3 edge for Pt/C were of very good quality and noise free modulations stretched up to 17 k starting from 2.2 k as shown in previous reports [22]. Figure 2 (b) shows the forward Fourier transforms of the EXAFS. As evident from this, both hydrogen and oxide regions induce changes in the magnitude of Pt-Pt interactions as evident from the differences in the magnitude of the Fourier transforms. As discussed in detail previously [22] the higher magnitude of the transforms at 0.0 V relative to 0.54 V was a result of a change in the morphology of the Pt nano-particles manifesting in changes in the coordination numbers (Table 2) while the Pt-Pt bond distance remained unchanged. At 0.84 V there was clear indication of the emergence of the oxide peak at 1.5 Å (Fig 2 (b)). The values of the coordination numbers and bond distances for the corresponding Pt-Pt and Pt-O interactions are given in Table 2. Figure 3 (a) shows the XANES at Pt L_3 edge for Pt/C in 1 M $HClO_4$ + 0.3 M MeOH. At 0.0 V there is a slight reduction in the white line near 0 eV and a slight widening at the higher energy side (5-10 ev above the edge) relative to the Pt foil standard, indicating the effect of adsorption of methanolic species at this potential and suppression of hydrogen adsorption. Such an adsorption effect at this potential has been reported previously based on electrochemical mass spectrometry [23] and electrochemical quartz crystal microbalance studies [24]. At 0.54 V, there is a significant increase in the white line intensity and broadening at the higher energy side of the spectrum. Comparison with similar measurements made with CO adsorbed on Pt/C has shown that this effect is primarily due to formation of CO on the surface and initiation of CO oxidation [25]. At 0.84 V, the onset of adsorption by oxygenated species becomes evident similar to the situation without methanol (Fig. 2 (a)). The corresponding Fourier transforms of the EXAFS at the Pt L_3 edge for Pt/C in the presence of MeOH reflect those seen in XANES (Fig. 3(b)). At 0.54 V there is lowering of the Pt-Pt interactions due to Pt-C interactions and the emergence of two peaks below 2 Å, which have been independently corroborated with CO adsorbed data [25]. At 0.84 V a further lowering of the Pt-Pt interactions due to adsorption of oxygenated species occurs manifested by the emergence of the Pt-O peaks at ~1.5Å. Hence based on the body of evidence presented so far it is clear that nano-particles of Pt supported on carbon are susceptible to perturbations in both electronic (Pt *5-d* band vacancies/atom) and geometric (coordination numbers) parameters due to adsorption of H, OH and C_1 containing organic species. It would thus be interesting to compare these results with corresponding analysis at the Pt L_3 and K edges of the second metal atom for PtRu and PtSn electrocatalysts to better understand its electrochemical characteristics.

3.3. XAS analysis of PtRu/C, PtSn/C and upd Sn on Pt/C at the Pt L and K edges of the second metal atom, Ru & Sn

Figure 4 (a) shows the XANES spectra for PtRu/C alloy at the Pt L_3 edge in 1 M $HClO_4$. Comparison of the spectra at 0.54 V (double layer region, hence no interference due to adsorption effects) with that of the Pt foil standard shows an increase in the white line intensity thereby indicating an increase in the Pt *5 d*-band vacancies/atom. In contrast to Pt/C, however, there is very little change in the white line as a function of potential for the alloy (similar particle size and carbon support). Calculated values of the Pt *5-d* band vacancies/atom (Table 2) reflect these observations. Forward Fourier transforms of the EXAFS at Pt L_3 edge also shows no change as a function of potential in contrast to the Pt/C electrocatalyst. This indicates that in contrast to

Pt/C, alloying of Pt with Ru renders it less susceptible to changes in the hydrogen and oxide regions in terms of both electronic and structural parameters except for an increased Pt *5-d* band vacancy as a result of alloying itself. These observations at the Pt L_3 edge are supported by similar conclusions on a series of binary alloys of Pt with first row transition elements ranging from Cr to Ni [19] and on PtRu/C electrocatalyst reported by us previously from Johnson Matthey (West Deptford, NJ, USA) [20]. Figure 5 (a) shows the XANES spectra at the Pt L_3 edge for PtSn/C alloy electrocatalyst in 1 M $HClO_4$. Unlike the case of alloying Ru with Pt, here the white line at 0.54 V is lower than the Pt foil reference standard, indicating thereby a filling of the Pt *5-d* band vacancies. Quantitative values of the Pt *5-d* band vacancies/atom are given in Table 2. This result is in contrast to all other transition elements studied including the binary alloys with first row transition series ranging from Cr to Ni [19]. Further, there is no effect on the white line as a function of potential, similar to PtRu/C alloy. Forward Fourier transforms of the EXAFS at Pt L_3 edge (Fig. 5(b)) also indicates very little change in potential range of 0.0 to 0.54 V (practical operating range for Sn containing electrocatalyst). Any discernible change appeared at significantly higher potentials such as 1 V (Fig 5 (b)), which is well beyond the stability region for Sn and the lowering of the Pt-Pt interactions seen in the Fourier transforms at this potential is a combination of Sn dissolution and the adsorption of oxygenated species on Pt surface. Results of the EXAFS analysis are given in Table 2, it shows increase in the Pt-Pt bond distance in contrast to PtRu/C alloy and other previously reported values on binary Pt alloys with first row transition elements [19]. The values also show a good agreement with those obtained from powder XRD measurements on the as received electrocatalysts. Figure 6 (a) shows the XANES at the Pt L_3 edge for Pt/C electrocatalyst with upd Sn on the surface (θ_{Sn}= 0.76). The spectra taken in the transmission mode does not indicate any perturbation of the electronic structure of Pt. However on a cautionary note, this spectra is averaged over the bulk of the crystallite and is not exclusive to the surface. Since the percent of surface atoms for a 35 Å particle is approximately 28 %, XANES in the transmission mode would pick up any significant changes, such as those resulting from adsorption of H, OH and C_1 species on the surface. Conducting these experiments in the fluorescence mode does not promise any improvements, since the depth of the fluorescence signal at the energy of Pt L edges is in the same order of magnitude as the particle size. For all practical purpose therefore the Pt electronic states do not appear to be significantly affected by upd Sn on the surface. It also does not cause any change in the structural characteristics (EXAFS data not shown), an expected result since upd deposition was not expected to cause any change in the bulk of the nano-crystallites. Figure 6 (c) shows the XANES spectra at the Sn K edge for the upd Sn on Pt/C in 1 M $HClO_4$. As evident from the figure, Sn appears to be always associated with oxygen at all potentials, even at 0.0 V, given its proximity to the SnO reference standard edge position instead of the Sn reference foil. The increase in the white line with potential from 0.0 to 0.54 indicates further nucleation of oxygenated species at higher potentials. Hence in the case of upd Sn on Pt/C, the enhanced electrocatalysis for MeOH oxidation appears to be primarily based on the ability of Sn to supply oxygenated species at very low potentials for oxidation of C_1 species formed on the surface. Since the Pt electronic and geometric parameters remain unchanged, it still possesses the ability to adsorb methanol via the first proton transfer, considered to be the rate determining step for MeOH oxidation on Pt [26]. Figure 7 (a) shows the XANES at the Sn K edge for PtSn/C alloy in 1 M $HClO_4$. The spectrum is very similar to that for upd Sn on Pt/C, thereby showing that in the alloy, Sn nucleates the oxygenated species at very low potentials, amount of which increases with potential. Hence the primary difference between the

upd and alloyed Sn on Pt appears to be the partial filling of the Pt *5 d*-band vacancies/atom and increase in the Pt-Pt bond distance as a result of alloying and their relative absence when Sn is added as a upd layer. The changes in the Pt *5 d*-band vacancy and bond distances as a result of alloying with Sn appears to have an adverse effect on the initial adsorption of MeOH (rate determining step). Such an effect is expected based on the Engel Brewer model for catalysis by transition elements [27]. Figure 7 (b) shows the XANES spectra at the Ru K edge for PtRu/C in 1 M $HClO_4$. Similar to the results at the Sn K, Ru appears to be associated with oxygenated species at low potentials such as 0.0 V, the amount of these species increase with potential. Hence, similar to Sn, Ru nucleates oxygenated species at potentials lower than Pt and is able to initiate oxidation of C_1 species on the surface at lower potentials. The advantage of alloying with Ru however is the increase in the Pt *5 d*-band vacancy and lowering of the Pt-Pt bond distance, which appears to be beneficial for the initial step of methanol adsorption (*rds*).

4. CONCLUSIONS

Based on the results presented in this paper, the following conclusions can be summarized as:

(a) Adsorption of hydrogen, oxygenated species and methanol oxidation products induce major changes in the Pt L edge XAS for Pt/C.
(b) Adsorption of hydrogen and oxygenated species appears to cause significantly lower changes in the Pt L_3 edge XAS for PtRu/C and PtSn/C.
(c) Ru, Sn in the alloy and upd Sn are associated with oxygenated species at all potentials and the amount and nature of these species are potential dependent.
(d) upd Sn does not appear to change the Pt *5 d*-states as well as cause any change in structural characteristics of Pt.
(e) Alloying of Sn to Pt causes filling of the Pt *5 d*-states and an increase in the Pt-Pt bond distance; alloying of Ru to Pt has just the opposite effect. These effects help explain the enhanced activities of MeOH oxidation by PtRu/C alloy. The higher *d*-band vacancy and lower Pt-Pt bond distances appear to be beneficial for the rate determining step involving the initial adsorption of methanol.

5. Acknowledgments

The authors gratefully acknowledge the support of the U. S. department of Energy, Division of Material Science, Brookhaven National laboratory (Contract # DEA-C02-76CH00016) for its role in the development and operation of the National Synchrotron Light Source (NSLS). The experimental work at Brookhaven was supported by the Office of Transportation Technologies, Electric and Hybrid Vehicles Division of D. O. E under contract # DEA-C02-76CH00016. The help of NIST personnel at beam line X23A2, Joseph Woicik is gratefully acknowledged.

REFERENCES

(1) B. D. McNicol, *J. Electroanal. Chem.*, **118**, 71 (1981).

(2) B. D. McNicol, in *Power Sources for Electric Vehicles,* B. D. McNicol and D. A. J. Rand, Editors, pp. 807-838, Elsevier, Amsterdam (1984).
(3) J.-M Léger and C. Lamy, *Ber. Bunsenges, Phys. Chem.*, **94**, 1021 (1990).
(4) R. Parsons and T. VanderNoot, *J. Electroanal. Chem.*, **257**, 9 (1988).
(5) K. Cathro, *J. Electrochem. Soc.*, **116**, 1608 (1969).
(6) M. M. P. Janssen and J. Moolhuysen: (a) *J. Catal.*, **46**, 289 (1977), (b) *Electrochimica Acta.*, **21**, 861 91976).
(7) M. R. Andrew, J. S. Drury, B. D. McNicol, C. Pinington and R. T. Short, *J. Appl. Electrochem.* **6**, 99 (1976).
(8) A. A. Mikhailova, N. V. Ostrova and Y. V. Vasil'ev, *Electrokhimiya*, **13**, 518 (1977).
(9) B. Bittens-Cattaneo and T. Iwasita, *J. Electroanal. Chem.*, **238**, 151 (1987).
(10) C. T. Hable, M. S. Wrighton, *Langmuir*, 7, 1305 (1991).
(11) M. Watanabe, Y. Furuchi and S. Motoo, *J. Electroanal. Chem.*, **191**, 367 (1985).
(12) A. Haner and P. N. Ross, *J. Phys. Chem.*, **95**, 3740 (1991).
(13) K. Wang, H. A. Gasteiger, N. M. Markovic and P. N. Ross, Jr., *Electrochimica Acta.*, **41**, 2587 (1996)
(14) S. A. Campbell and R. Parsons., *J. Chem. Soc. Faraday Trans.*, **88(6)**, 833 (1992).
(15) A. S. Arico, V. Antonucci, N. Giordano, A. K. Shukla, M. K. Ravikumar, A. Roy, S. R. Barman and D. D. Sarma, *J. Power Sources,* **50**, 295 (1994).
(16) H. A. Gasteiger, N. M. Markovic and P. N. Ross, Jr., *J. Phys. Chem.*, **99**, 8945 (1995).
(17) T. R. Thurston, N. M. Jisrawi, S. Mukerjee, X. Q. Yang, J. McBreen, M. L. Daroux, and X. K. Xing, *Appl. Phys. Lett.*, **69**, 194 (1996).
(18) J. McBreen, W. E.O'Grady, K. I. Pandya, R. W. Hoffman and D. E. Sayers, *Langmuir*, **3**, 428 (1987).
(19) S. Mukerjee, S. Srinivasan, M. P. Soriaga and J. McBreen, *J. Electrochem. Soc.*, **142**, 1409 (1995).
(20) J. McBreen and S. Mukerjee, *J. Electrochem. Soc.*, **142**, 3399 (1995).
(21) D. Aberdam, R. Durand, R. Faure, F. Gluaguen, J. L. Hazemann, E. Herrero, A. Kabbabi, O. Ulrich, *J. Electroanal. Chem.*, **398**, 43 (1995).
(22) S. Mukerjee and J. McBreen, *J. Eelctrochem. Soc.*, **143**, 2285 (1996).
(23) M. Krausa and W. Vielstich, *J. Electroanal. Chem.*, **379**, 307 (1994).
(24) C. P. Wilde and M. Zhang, *Electrochim. Acta.*, **39**, 347 (1994).
(25) J. McBreen and S. Mukerjee, *Extended Abstracts for the 190th Meeting of the Electrochemical Society, San Antonio, Texas, October 6-11,* 1996.
(26) P. S. Krausen, E. Skou and J. Munk, *J. Electroanal. Chem.*, **404**, 1 (1996).
(27) L. Brewer in *Phase Stability in Metals and Alloys,* (P. Rudman, J. Stringer, and R. Jafee Edirors), McGraw Hill, New York (1967) pp39.

DISCLAIMER

TABLE 1: RESULTS OF POWDER X-RAY DIFFRACTION STUDIES ON Pt AND Pt ALLOYS

Electrocatalyst	Lattice Parameter (Å) (Pt-Pt Bond distance, (Å)	Particle Size (Å)
Pt/C	3.927 (2.777)	35
PtSn/C	4.0015 (2.829)	34
PtRu/C	3.8907 (2.751)	35

TABLE 2 : RESULTS OF XANES AND EXAFS ANALYSIS AT THE Pt L_3 EDGE FOR PtC, PtRu/C AND PtSn/C ALLOY ELECTROCATALYSTS AT 0.0, 0.54 AND 0.84 V vs RHE IN 1 M $HClO_4$

Pt/C

Electrode Potential (V)	Pt *5-d* band vacancy/atom	Shell	EXAFS Parameters			
			N	R(Å)	$\Delta\sigma^2$ (Å^2)	ΔE_o(eV)
0.0	0.335	Pt-Pt	10.64	2.772	0.0044	0.93
0.54	0.329	Pt-Pt	8.66	2.773	0.0044	-0.88
0.84	0.370	Pt-Pt	6.73	2.773	0.0048	-0.20
		Pt-O	1.69	2.039	0.0042	2.48

PtRu/C

Electrode Potential (V)	Pt *5-d* band vacancy/atom	Shell	EXAFS Parameters			
			N	R(Å)	$\Delta\sigma^2$ (Å^2)	ΔE_o(eV)
0.0	0.378	Pt-Pt	7.51	2.73	0.00050	3.49
		Pt-Ru	2.16	2.69	0.00164	-6.28
0.54	0.382	Pt-Pt	7.52	2.73	0.0052	2.07
		Pt-Ru	2.61	2.69	0.0028	-6.24
0.84	0.388	Pt-Pt	7.49	2.73	0.0052	3.36
		Pt-Ru	2.74	2.69	0.0029	-4.46

PtSn/C

Electrode Potential (V)	Pt *5-d* band vacancy/atom	Shell	EXAFS Parameters			
			N	R(Å)	$\Delta\sigma^2$ (Å^2)	ΔE_o(eV)
0.0	0.298	Pt-Pt	8.24	2.801	0.0055	2.91
		Pt-Sn	2.56	2.803	0.0132	-5.75
0.54	0.296	Pt-Pt	7.89	2.801	0.0051	3.55
		Pt-Sn	2.83	2.800	0.0097	-5.63
0.84	0.297	Pt-Pt	7.88	2.798	0.0052	4.20
		Pt-Sn	2.89	2.796	0.0089	-5.244

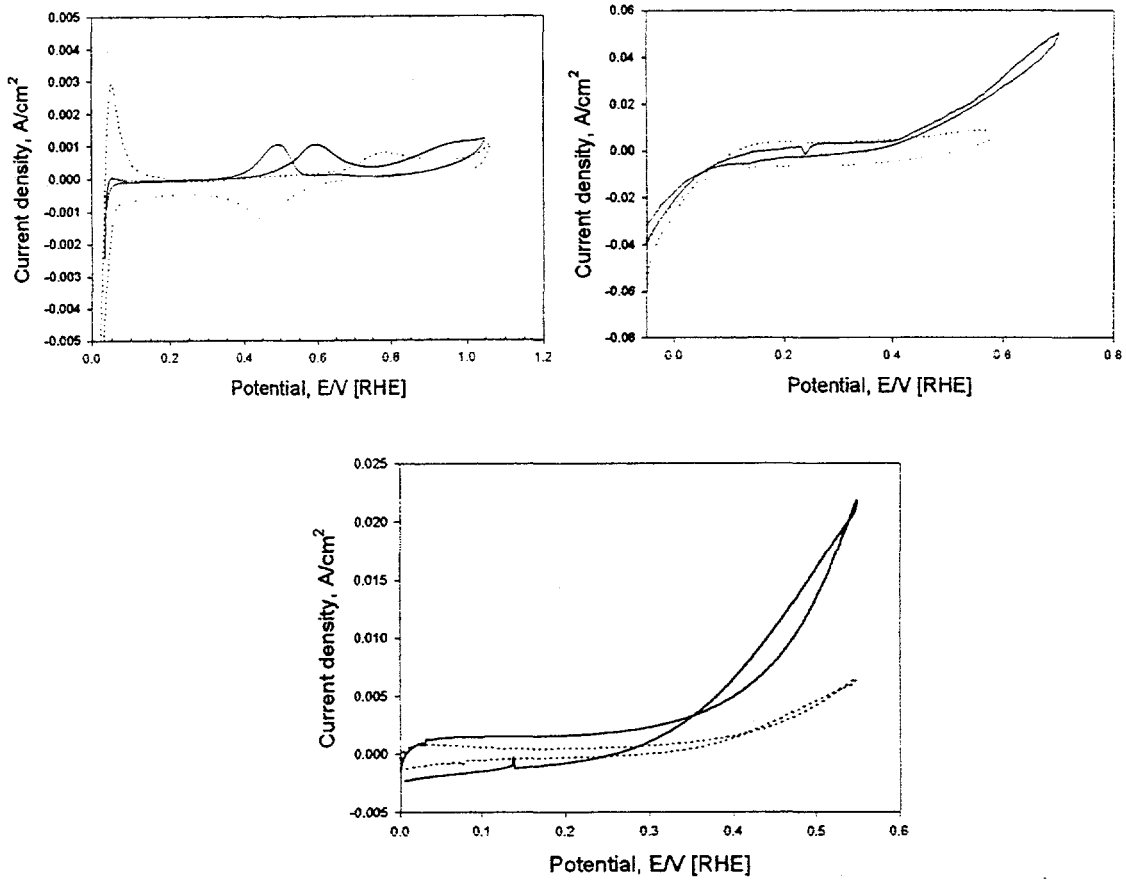

Figure 1. Cyclic voltammograms for (a) Pt/C , (b) PtRu/C alloy with (—) and without (...) 0.3 M MeOH in 1 M $HClO_4$ and (c) PtSn/C alloy (...) and upd Sn on Pt/C (—) in 1 M $HClO_4$ + 0.3M MeOH. All CV's taken in *in situ* spectro-electrochemical cells at a scan rate of 2mV/s.

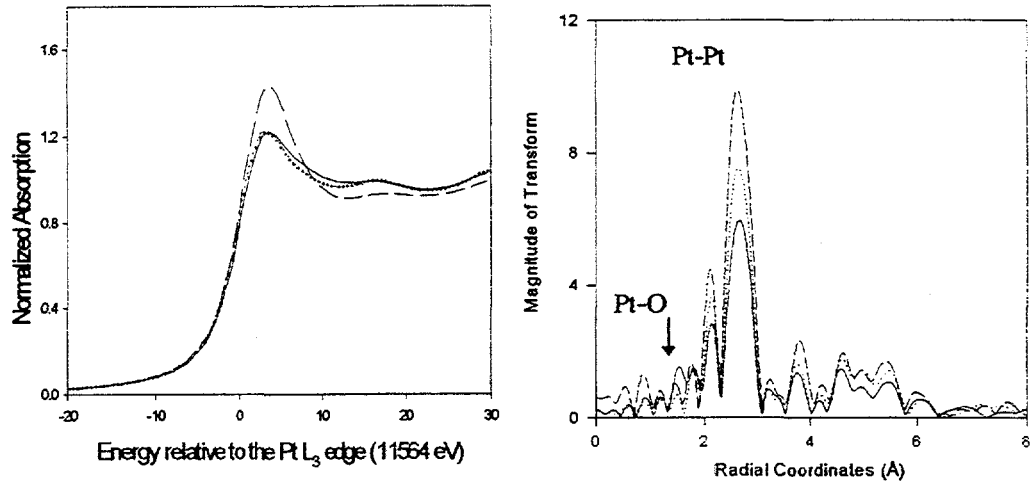

Figure 2. XAS at the Pt L_3 edge for Pt/C in 1 M $HClO_4$ showing (a) XANES at 0.0 (—), 0.54 (...) and 0.84 V vs RHE (---) vs pure Pt reference foil (+) and (b) EXAFS at 0.0 (---), 0.54 (...) and 0.84 V (—) vs RHE.

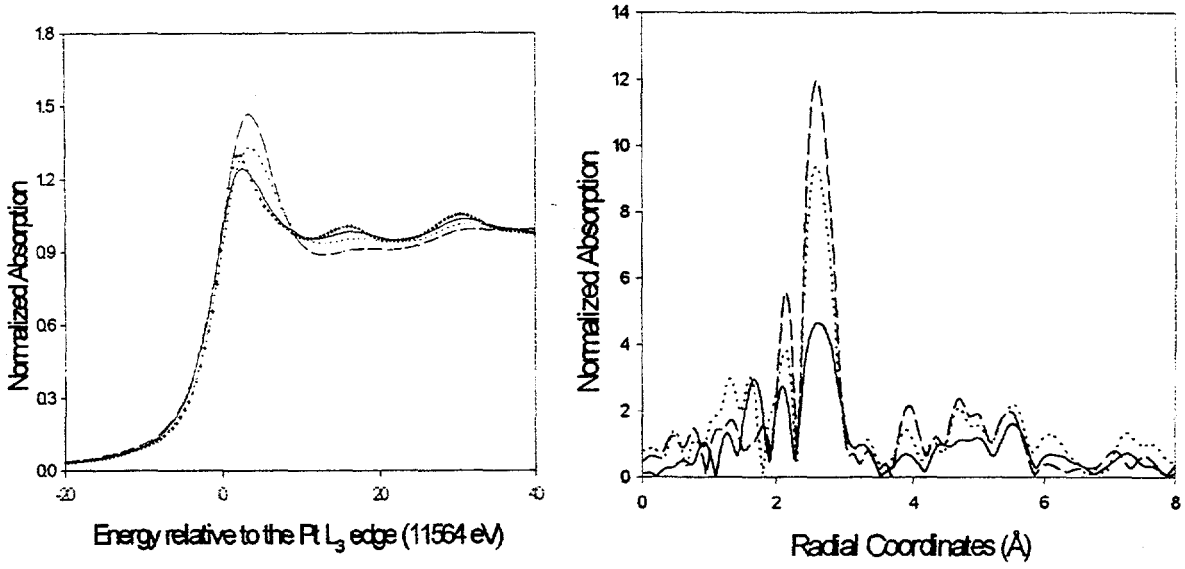

Figure 3. XAS at the Pt L_3 edge for Pt/C in 1 M $HClO_4$ + 0.3 M MeOH, (a) XANES at 0.0 (—), 0.54 (...) and 0.84 (---) vs RHE relative to a Pt reference foil (+) and (b) Fourier transforms of the EXAFS at 0.0 (---), 0.54 (...) and 0.84 (—) V vs RHE.

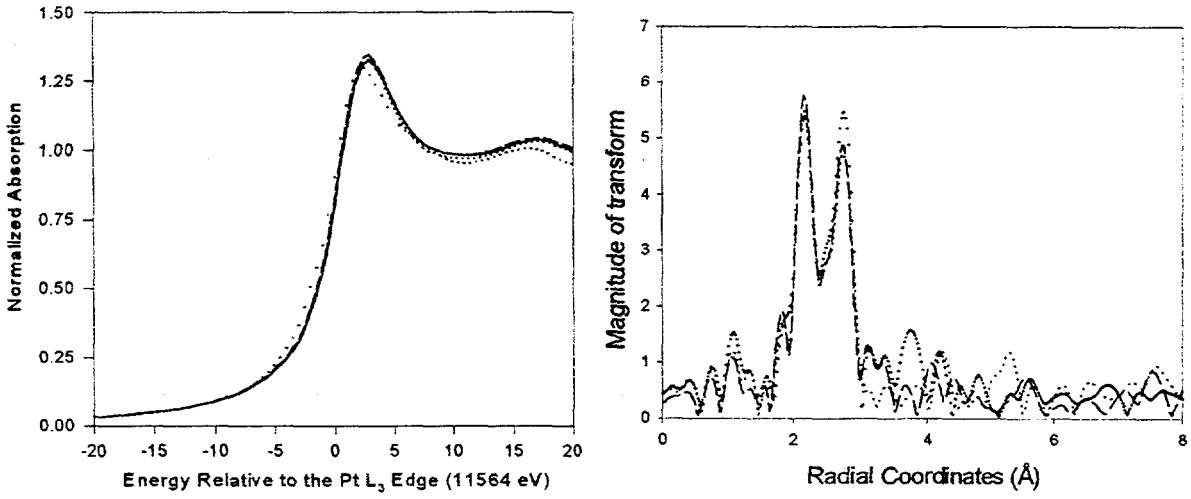

Figure 4. XAS at the Pt L_3 edge for PtRu/C alloy in 1 M $HClO_4$, (a) XANES at 0.0 (—), 0.54 (...) and 0.84 V (---) vs RHE relative to a Pt reference foil (+) and (b) Fourier transform of the EXAFS at 0.0 (---), 0.54 (...) and 0.7 V (+) vs RHE.

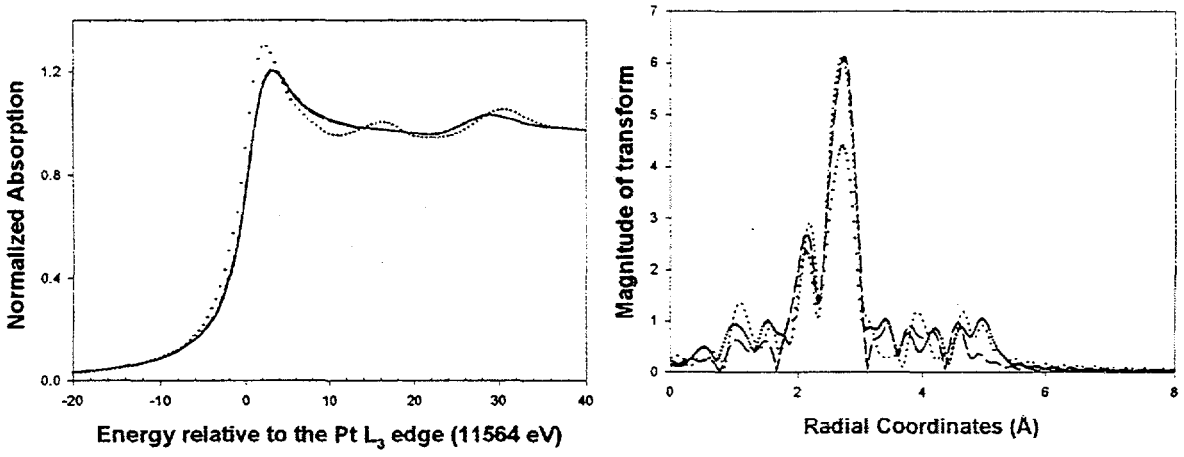

Figure 5. XAS at the Pt L_3 edge for PtSn/C alloy, (a) XANES at 0.0 (—), 0.54 (...) and 0.84 v (- -) vs RHE relative to Pt reference foil (+) and (b) Fourier transforms at 0.0 (---), 0.54 (...) and 1.0 (+) V vs RHE.

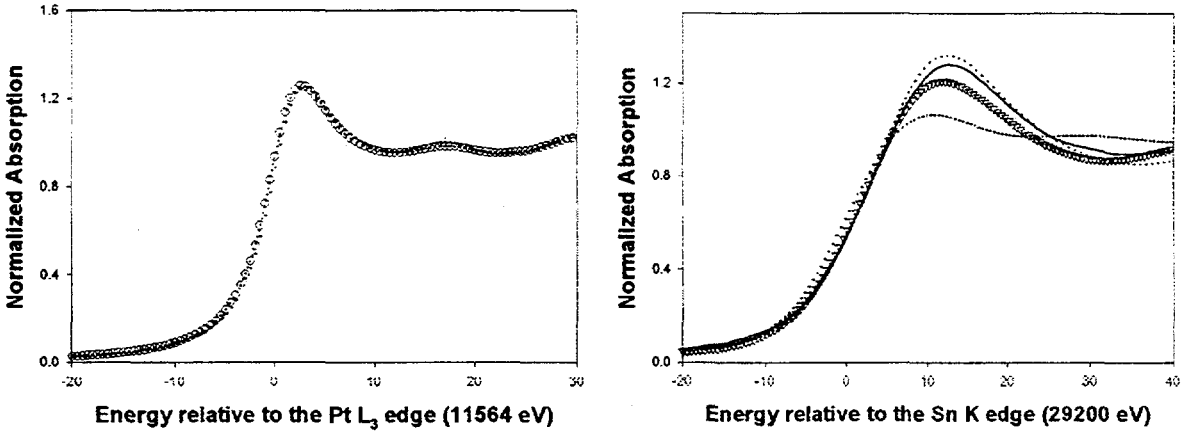

Figure 6. Upd Sn on Pt/C in 1 M $HClO_4$, (a) XANES at the Pt L_3 edge 0.33 (O), 0.54 (...) V vs RHE relative to a Pt reference foil (+) and (b) XANES at Sn K edge, 0.0 (—), 0.54 (...) V vs RHE relative to Sn (+) and SnO (Δ) reference foil.

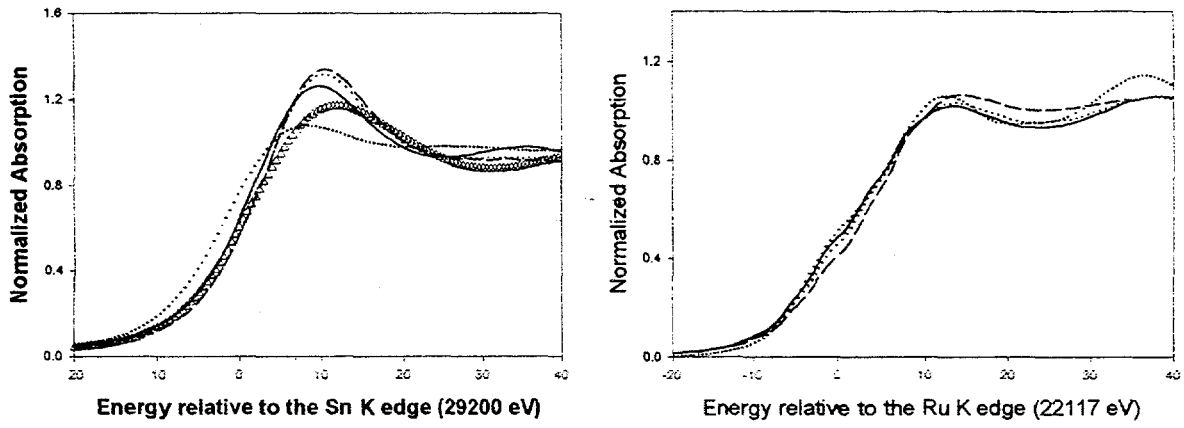

Figure 7. XANES at (a) Sn K edge for PtSn/C alloy in 1 M $HClO_4$ at 0.0 (—), 0.54 (...) and 0.84 (---) V vs RHE relative to Sn (+) and SnO (Δ) reference standards and (b) Ru K edge XANES for PtRu/C in 1 M $HClO_4$ at 0.0 (—), 0.54 (...) and 0.84 (---) V vs RHE relative to Ru black reference standard (+).